

Fig. 1. (a) Geological map of the Altai region in Mongolia and China, showing the distribution of various tectonic units and structures. (b) Detailed view of the Fuyun-Daogui region. The map is based on data from *et al. 200*.

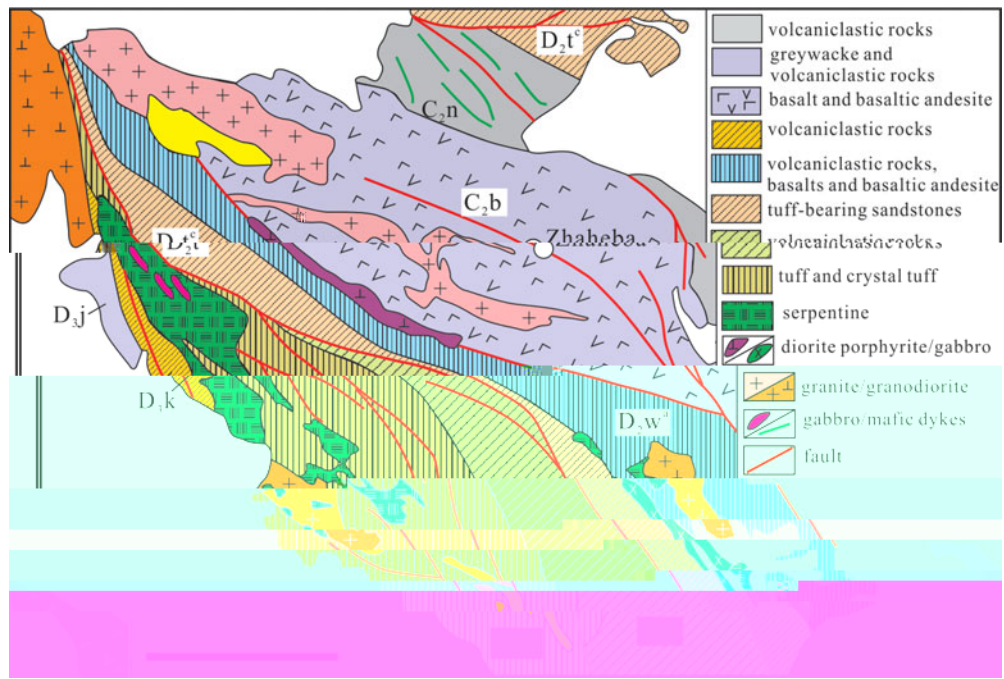
The Altai region is characterized by a complex tectonic history. The Altai Mountains are a major tectonic feature, formed by the collision of the Siberian Craton and the North China Craton. The region is divided into several tectonic units, including the Altai Mountains, the Fuyun-Daogui region, and the Keketuohai complex. The Altai Mountains are composed of various rock units, including gabbro, diorite, and quartz diorite. The Fuyun-Daogui region is characterized by a sequence of volcanic and sedimentary rocks. The Keketuohai complex is a large igneous province, consisting of a variety of igneous rocks, including gabbro, diorite, and quartz diorite.

The Altai region is characterized by a complex tectonic history. The Altai Mountains are a major tectonic feature, formed by the collision of the Siberian Craton and the North China Craton. The region is divided into several tectonic units, including the Altai Mountains, the Fuyun-Daogui region, and the Keketuohai complex. The Altai Mountains are composed of various rock units, including gabbro, diorite, and quartz diorite. The Fuyun-Daogui region is characterized by a sequence of volcanic and sedimentary rocks. The Keketuohai complex is a large igneous province, consisting of a variety of igneous rocks, including gabbro, diorite, and quartz diorite.

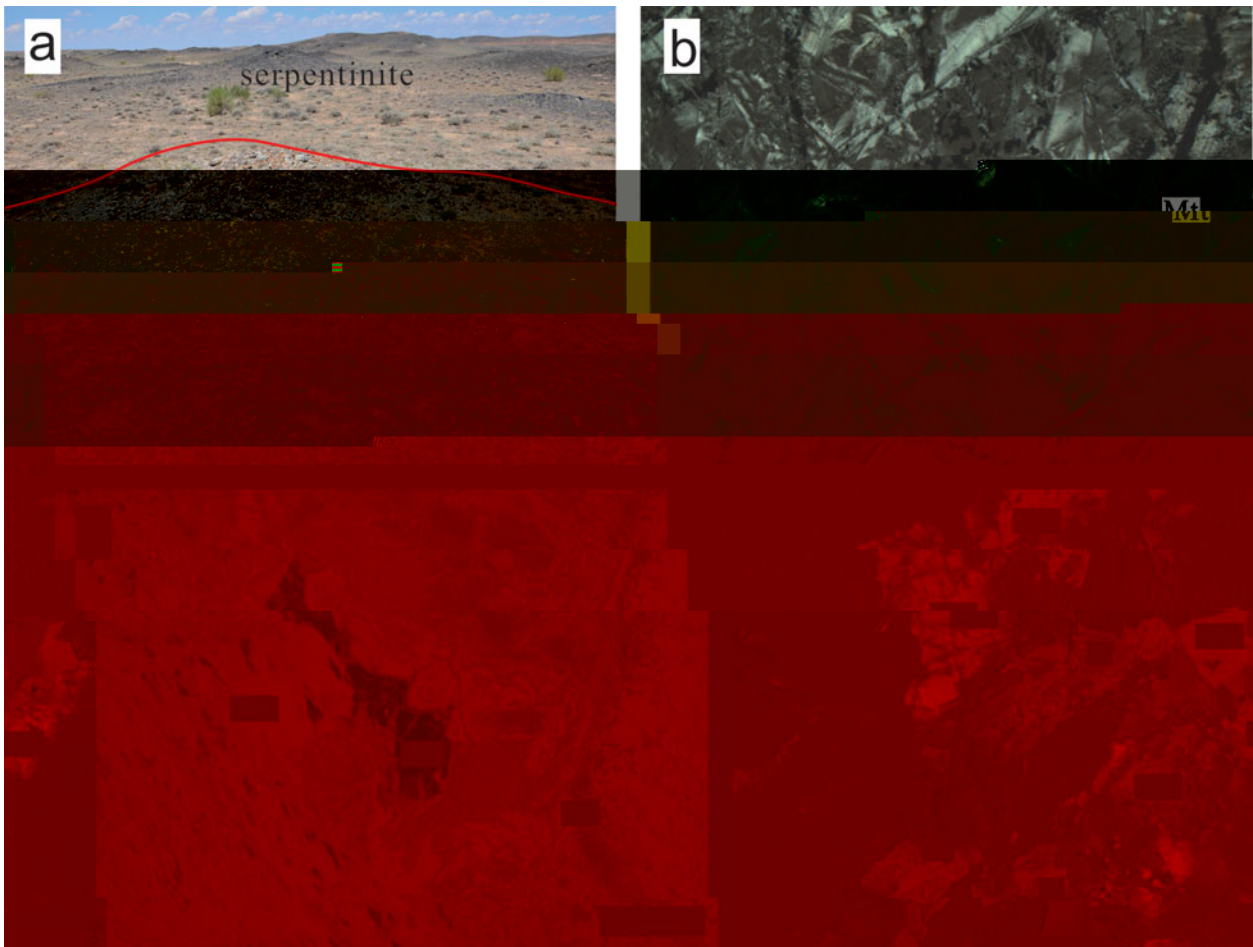
2. Regional geology, field observations and petrography

The Altai region is characterized by a complex tectonic history. The Altai Mountains are a major tectonic feature, formed by the collision of the Siberian Craton and the North China Craton. The region is divided into several tectonic units, including the Altai Mountains, the Fuyun-Daogui region, and the Keketuohai complex. The Altai Mountains are composed of various rock units, including gabbro, diorite, and quartz diorite. The Fuyun-Daogui region is characterized by a sequence of volcanic and sedimentary rocks. The Keketuohai complex is a large igneous province, consisting of a variety of igneous rocks, including gabbro, diorite, and quartz diorite.

The Altai region is characterized by a complex tectonic history. The Altai Mountains are a major tectonic feature, formed by the collision of the Siberian Craton and the North China Craton. The region is divided into several tectonic units, including the Altai Mountains, the Fuyun-Daogui region, and the Keketuohai complex. The Altai Mountains are composed of various rock units, including gabbro, diorite, and quartz diorite. The Fuyun-Daogui region is characterized by a sequence of volcanic and sedimentary rocks. The Keketuohai complex is a large igneous province, consisting of a variety of igneous rocks, including gabbro, diorite, and quartz diorite.



e2. (e) e ca a e a e a e c e (e a e et al. 2007, 200 a a a , 1 3).



e3. (e) e a a c c c a e e e e e a e a e. (a) ae e e e c e a . (, c) e e e e c e > 0% e e ea a e e a e. () e a a c e a ca e, c e ea e e. c e e, a e e, a ca e, e, e e e.

a a e v ca c e e a a a e -
e ve ae c e e e.

3. Analytical procedures

3.a. Zircon U-Pb dating and Hf-O isotope analysis

c e e e a a e a a a e
(2013 01, 46°32'51", 8°24') a a
a e (2013 02, 46°33'2", 8°23'36") c ec-
e e e a e e e e e e .
c e a a a ca e c ve a
a e ca e ec e. c a ee
e a - ce e a c a c c e. c
a a c e e e ce a a ee e
e ec a , c ee e e ec
ec a a a . c ee c ee
a e a e e ce c a a e
a ca e ce ce () a e e ve a e
e a c e. c a e a ec -
e e a a e e a e a a c -
ve c e a a a ec e (- -)
e a e a e e a e a
e ce , ee e ca ve . e e a e
a a ca ce e ave ee c ee e
et al. (2011). e e e a a e e a e
a e e e a a e . a a e c
a e e - e - a a a (et al.
2010) a (, 2003). e e e ea
a e a e e a e 5% c e ce eve . c
a e a a a ec a e e
e e e a a e a a e 1 a e
e e a a e a a e 2, e ec ve , a va -
a ea .// a .ca e. / e .
c e e ee ea e e
a e ca 1280 a e e e a
e c , ee ca e ce ce e ,
a a ca ce e a e e e
et al. (2010a). ea e ¹⁸ / ¹⁶ a ee
a e e a a a ea cea
a e c (, ¹⁸ / ¹⁶ = 0.0020052),
a e c e ce e e a a ac -
a ac () e a c a a ee -
e ce a a a δ¹⁸ va e 5.31‰ (et al.
2010b). e ea e e e c a -
a ea δ¹⁸ e c e e a e e
ea δ¹⁸ 5.44 ± 0.21‰ (2), c c -
e e e ee e va e 5.4 ± 0.2‰
(et al. 2013). c e c a a e e
e e e a a e a a e 3 a va a ea
.// a .ca e. / e .

3.b. Mineral analysis

e a c ee ee e e
- ec a a ae 8800 e ec-
c e e e ve ave e
ec ee a e a e e ce -
, ee ca e ce ce . ea c -
ee 15 e acce ea v a ea 15

ea c e 20 c e. e ee -
a ve ea ca a a e e e -
e e a ae a a e 4 a 5 a va a e a
.// a .ca e. / e .

3.c. Whole-rock analysis

e- c a - a ace-ee e c
e e a e a e a e e e ce -
, ee ca e ce ce . a ee e
e e a e a a 100e -
e a a ca ce e ec e et al.
(2004). a ca ec e e a e e a
2%. ace ee e e e a e a e -
e ce e 6000 - ce -
e ec e et al. (2004). 50
a e e eac a e ee ve
- e e e a + 3 -
e. e a a a c a e
ee e a e a a e
c . e a a -1, -2 a -2,
a e ee a a a a -1 a -
3, ee e ca a ee e c ce a
ea e a e. - a a ca ec
ee e a ee a 3 5%. e a a ca e
a e a e 1.
a e c ea e e ee
e a ve e + 3
ac , a e e a a e c ve a ca -
e ca e ec e. e c ea e e ee
e e a c a e -c ec
c ve c e a a a ec ee (-
-) a e ae e a a e e-
e ce , e e ce , ee
ca e ce ce . e ea e ce e a ee
ec e et al. (2004). e ea e ⁸⁷ / ⁸⁶
a ¹⁴³ / ¹⁴⁴ a a e c e ce ⁸⁶ / ⁸⁸ =
0.114 a ¹⁴⁶ / ¹⁴⁴ = 0.721 , e ec ve . e
ea e ⁸⁷ / ⁸⁶ ave a e a ee 0.710288
e ⁸⁷ a a a 0.70506 -1, a
e ¹⁴³ / ¹⁴⁴ ave a e a ee 0.512104 -
1 a 0.512671 -1. e a a ca e a
c a e a a e e e a e 2.

4. Analytical results

4.a. Zircon U-Pb ages

c e a a e a e a ce a
c e . a ae ac e
a 100 150 μ a a ec a a
1.1 2.1. a e , e c a
e c a , ea e c a ace c -
c a c a a c c (ee e .4a).
a a e e ec ce a e , a
e e va a e (22 123) a (8
57) c e / a a 0.4
0.8. e - eve a a e 30 c e e
c e e ac c a a e a a -
ca e a a e e ea a e 485.8 ± 2.5 a

a e l. e

a e c	2013	01-1	2013	01-3	2013	01-4	2013	01-5	2013	01-6	2013	01-7	2013	01-8	2013	01 1	2013	01 2	2013	01 4	
	0.005		0.064		0.008		0.005		0.00		0.003		0.003		0.051		0.044		0.222		
	0.021		0.347		0.044		0.042		0.072		0.031		0.033		0.310		0.257		1.450		
	0.004		0.047		0.007		0.008		0.011		0.005		0.005		0.04		0.043		0.21		
	0.011		0.232		0.036		0.044		0.012		0.034		0.008		0.123		0.0 0		0. 3		
a	0.0 0		0.036		0.038		0.037		0.068		0.026		0.025		0.046		0.031		0.067		
	0.268		1.710		6.600		1.880		0. 3		0.233		1.150		1.570		0.516		0.1 5		
	0.406		0.0 2		0.127		0.112		0.0		0.1		0.054		0.168		0.1 1		0.6 5		
	0.046		0.034		0.014		0.028		0.050		0.030		0.010		0.050		0.02		0.130		
	0.1 1		0.144		0.203		0.364		0.042		0.0 4		0.07		0.066		0.042		0.073		
a e c	2013	01 5	2013	01 6	2013	01 7	2013	01 8	2013	01	2013	03 2	2013	03 3	2013	03 4	2013	03 5	2013	01 3	
			(1)		(1)		(1)		(1)		(1)		(1)		(1)		(1)		(1)		(2)
			<i>Major elements (%)</i>																		
2	4 .17		45.87		48.7		53.1		51. 1		50.40		50.54		50.52		51.22		52.37		
2	0.34		0.15		1.40		1.24		1.31		1.70		1.63		1.31		1.17		0.33		
2 3	18.		1 .58		16.5		16.1		15. 3		15.87		16.76		15.55		15.48		1 .61		
e2 3	4.52		3.34		7.88		7.11		7.43		.0		.50		.42		7.82		3.44		
	0.0		0.08		0.11		0.10		0.11		0.13		0.11		0.14		0.12		0.07		
	6.87		7.42		4.80		4.28		4.41		5.8		3.2		6.06		7.14		4.88		
a	11.03		12.61		6.22		5.75		6.3		6.75		4.52		7.4		8.26		8. 0		
a2	4.86		7.38		8.72		8.3		8.00		4.52		7.31		4.80		4.08		7.11		
2	0.13		0.11		0.3		0.31		0.42		2.04		0.33		1.27		2.03		0.17		
2 5	0.04		0.02		0.62		0.62		0.65		0.74		0.6		0.47		0.44		0.04		
	3.72		3.26		4.24		2.54		2. 3		2.27		5.14		2.65		1. 3		2.7		
	.75		.82		.76		.70		.4		.40		.81		.67		.68		.71		
	4. 8		7.4		.11		8.70		8.42		6.56		7.64		6.07		6.11		7.2		
#	75		81		55		54		54		56		41		56		64		74		
			<i>Trace elements (ppm)</i>																		
e	.0		4. 5		1.16		1.12		1.47		.08		40.4		5.2		6.82		5.71		
c	0.22		0.135		1.284		1.683		1.316		1. 53		1.034		1.100		0.575		0.62		
	25.0		23.8		18.6		17.5		17.5		7.5		1 .2		25.2		18.		17.0		
	118		83.7		186		166		172		227		22		254		187		75.7		
	34.7		163		60.5		62.6		64.1		116		18.		0.7		203		23.7		
	24.2		21.6		26.		23.6		24.6		27.8		28.5		28.0		28.0		16.4		
	4.7		175		63.6		50.7		51.4		76.8		27.7		57.3		132		71.1		

a e l. e		2013 01 5	2013 01 6	2013 01 7	2013 01 8	2013 01	2013 03 2	2013 03 3	2013 03 4	2013 03 5	2013 01 3
a	e			(1)	(1)	(1)	(1)	(1)	(1)	(1)	(2)
a	e	3. 7	1.20	3 .60	46.70	47.30	23.40	43.00	25.20	32. 0	6.56

a e l. e		2013	01 11	2013	02 1	2013	02 2	2013	03 1	2013	03 6	2013	01 10	04 06	04 24	04 2	03 17
a e c e		(2)		(2)		(2)		(1)	(1)	(2)		(1)	(1)	(1)	(1)	(1)	
<i>Trace elements (ppm)</i>																	
e c		1 .4		36.		42.4		26.0		32.4		17.		/	/	/	/
		0.3 5		0.153		0.358		1.1 8		0. 47		0.468		/	/	/	/
		32.5		33.2		34.5		25.1		26.3		32.1		13.4	20.5	17.7	20.3
		1 4		203		217		337		341		1 5		144	184	214	265
		56.5		44.2		47.8		1 .8		22.2		53.8		158	162	214	265
		34.7		37.5		38.3		23.1		24.8		33.8		20.6	30.	28.	20.2
		66.4		84.6		76.4		25.4		27.1		66.6		8 .1	114	75.5	7.02
		6.4		236.4		256.7		205.4		208.		114.20		/	/	/	/
		48.0		44.1		4 .0		4.		103		44.1		/	/	/	/
		12.0		11.1		11.2		14.7		13.6		12.0		/	/	/	/
a		0.58		1.420		1.070		3.130		3.270		0.583		4.	18.1	22.0	17.2
		71		1750		5		270		24		686		71	831	1118	776
		13.0		13.0		13.2		21.1		22.		12.5		13.2	13.2	14.7	20.1
		54.		42.3		41.5		144		154		52.8		243	133	164	151
		1.2		0.847		0.855		11.315		11. 85		1.257		20.2	12.7	21.	12.2
		0.025		0.030		0.027		0.051		0.052		0.028		/	/	/	/
		0.381		0.286		0.328		1.560		1.450		0.360		/	/	/	/
		0.288		1.720		1.030		0.365		0.406		0.336		/	/	/	/
		117		372		346		825		507		84.3		/	/	/	/
		10.70		7.840		7.610		26.40		26.80		10.50		30.6	32.2	40.1	26.4
a e		23.00		18. 0		18.40		51.50		54.70		22.30		57.8	62.	82.3	52.5
		2.770		2.520		2.510		5.750		6.180		2.670		6. 7	7.84	10.5	6.4
		11.80		11.70		11.60		22.30		24.30		11.60		27.5	31.2	43.1	24.4
		2.540		2.700		2.6 0		4.4 0		4.700		2.370		4.5	5.28	6.8	4.85
		0.8 6		0. 18		0. 70		1.163		1.257		0.883		1.45	1.58	2.07	1.03
		2.480		2.813		2.754		4.14		4.46		2.522		3.56	4.01	5.35	4.23
		0.3 6		0.38		0.3 7		0.612		0.660		0.384		0.4	0.54	0.64	0.63
		2.180		2.150		2.220		3.420		3.680		2.130		2.57	2.77	3.24	3.75
		0.468		0.446		0.444		0.728		0.75		0.468		0.4	0.52	0.5	0.78
		1.350		1.230		1.240		2.120		2.2 0		1.310		1.32	1.37	1.45	2.25
a		0.1 0		0.16		0.175		0.304		0.328		0.1 4		0.1	0.2	0.2	0.34
		1.210		1.050		1.120		1. 60		2.110		1.210		1.25	1.23	1.24	2.13
		0.174		0.164		0.165		0.2 1		0.323		0.173		0.20	0.17	0.17	0.34
		1.3 0		0. 41		1.040		3.2 0		3.510		1.460		5.37	3.27	4.16	3.72
		0.084		0.062		0.051		0.5 7		0.644		0.07		1.35	0.68	1.16	0.68
		0.151		2.0		1.50		2.75		1.88		0.33		/	/	/	/
		0.3 4		0.206		0.200		45.20		35.10		0.417		8.13	8.07	4.18	21.06
		1. 0		0.761		0.717		8.860		.2 0		1. 80		4.50	2.63	3.20	.41
		0.500		0.304		0.302		2.830		3.480		0.501		1.7	0.67	1.46	2.5

e. e e e a , a a , a a c a e e / e e e c .
 a a a e 04 06, 04 26, 04 2 a 04 17 a e et al. (200 a).

a e 2.	c c	e a a	e a e a e a	$^{87}\text{Sr}/^{86}\text{Sr}$	$^{87}\text{Sr}/^{86}\text{Sr}$ (1σ)	$^{87}\text{Sr}/^{86}\text{Sr}$	$^{147}\text{Sm}/^{144}\text{Sm}$	$^{143}\text{Nd}/^{144}\text{Nd}$	$^{143}\text{Nd}/^{144}\text{Nd}$ (1σ)	$^{143}\text{Nd}/^{144}\text{Nd}$	$\epsilon(t)$		
2013	01 3	a a (2)	0.36	3 2	0.0027	0.704030(2)	0.704015	2.4	10.8	0.13 4	0.51283 (40)	0.512474	6.
2013	01 10	a a (2)	0.58	686	0.0024	0.70475 (23)	0.704745	2.37	11.6	0.1235	0.51280 (43)	0.512486	7.1
2013	03 1	a a (1)	3.13	270	0.0335	0.706324(20)	0.706133	4.4	22.3	0.1217	0.512533(47)	0.512214	1.8
2013	03 2	a a (1)	2.87	1320	0.0063	0.70428 (20)	0.704255	4.5	28.6	0.1046	0.51271 (51)	0.512445	6.3
2013	03 3	a a (1)	8.06	516	0.0452	0.705368(43)	0.705111	5.7	36.	0.078	0.512707(30)	0.512450	6.4
2013	03 4	a a (1)	.65	1480	0.018	0.704227(51)	0.704120	4.55	24.5	0.1123	0.512803(53)	0.51250	7.5

$\epsilon(t) = 10000((^{143}\text{Nd}/^{144}\text{Nd})_t / (^{143}\text{Nd}/^{144}\text{Nd})_{401}) - 1$, $\epsilon(t) = (^{87}\text{Sr}/^{86}\text{Sr})_t - (^{87}\text{Sr}/^{86}\text{Sr})_{401}$

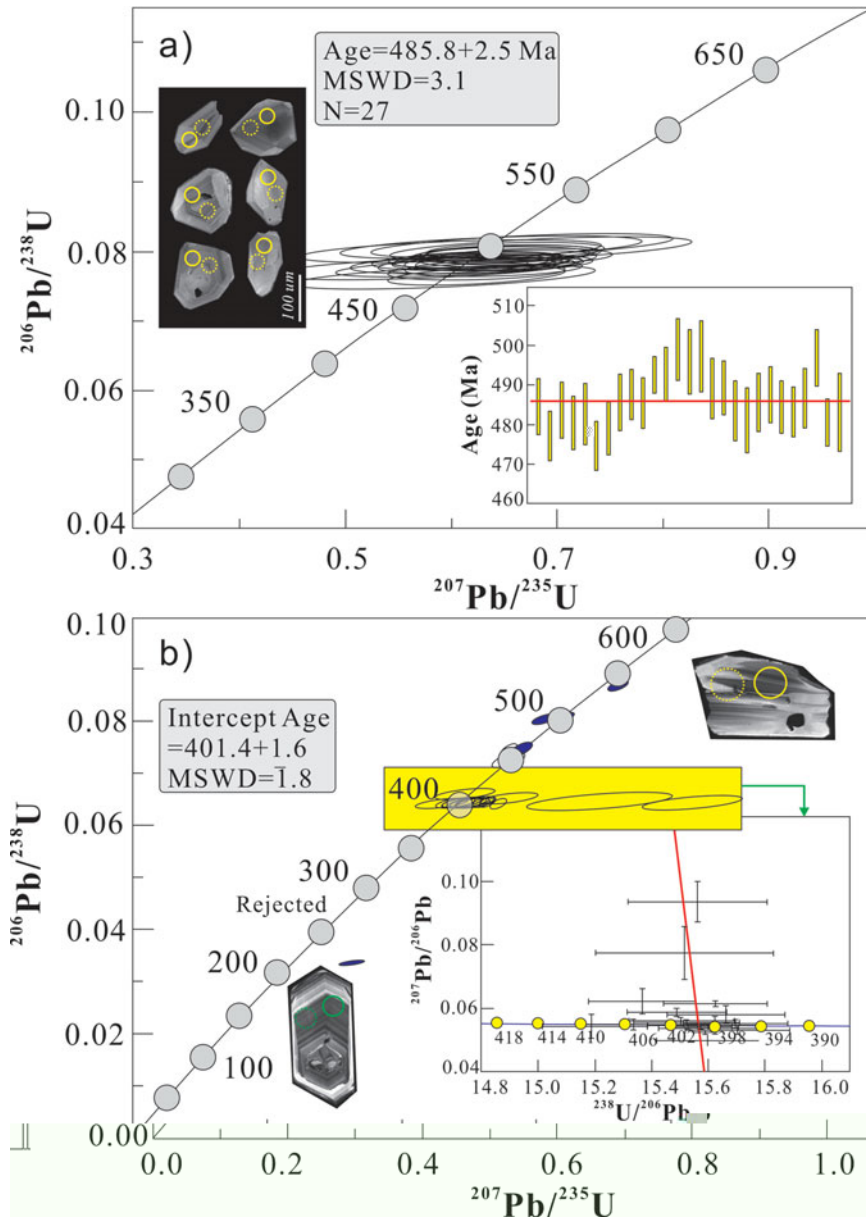


Fig. 4. (a) $^{206}\text{Pb}/^{238}\text{U}$ vs $^{207}\text{Pb}/^{235}\text{U}$ concordia diagram for the Zhaheba ophiolite. The age of the concordia intercept is 485.8 ± 2.5 Ma (MSWD = 3.1, N = 27). (b) $^{206}\text{Pb}/^{238}\text{U}$ vs $^{207}\text{Pb}/^{235}\text{U}$ discordia diagram for the Zhaheba ophiolite. The intercept age is 401.4 ± 1.6 Ma (MSWD = 1.8). The shaded area represents the discordance zone. The inset images show zircon grains used for dating.

(Fig. 4a, $n = 27$, $\text{MSWD} = 3.1$). The age of the concordia intercept is 485.8 ± 2.5 Ma. The age of the discordia intercept is 401.4 ± 1.6 Ma. The discordance zone is shaded in yellow. The inset images show zircon grains used for dating.

ca, a ea e c c -
 a e cc a a (2, ee e .4).
 e - ea a e ee e e c
 e a e. ee, e e 2
 c e e e a e a 450 a
 500 a a a e e e e c . e e
 21 a a e e e e 1 c e c -
 e ²⁰⁶ ²³⁸ a e a e e ea a e
 401 ± 2 a (= 3.3). e c a ce
 e ee ²⁰⁶ ²³⁸ a e a ²⁰⁷ ²³⁵ a e, e ea-
 a e ve e c a a a e a e
 e ce a e 401.4 ± 1.6 a (= 1.8) (ee
 e .4), c c c e e ²⁰⁶
²³⁸ e e ea a e. a e c e e
 eca a e(a , 1 3).

4.b. Mineral compositions

4.b.1. Spinel composition

cce c a e cc e e e e
 (.3). a a e 100 300 μ ac . e
 a a ca e (e e e a a e a a e
 4ava a ea .// a .ca e. / e)
 a e e ave 2 3, e a 2 3 c -
 e , va a e , a a 2 c e .
 e ea ce a ee a e
 a e c a e . (100 / (+))
 a 44 60 a . (100 / (+ e))
 25 61. ec a va a c e
 e e ae a e e / c eac a /
 - a a c ce (et al. 2010). e eve
 ace e e e e ve e ac -
 ca ee eec () a e e
 e e ac e e ee ace e e a e
 e e(a et al. 2013).

4.b.2. Pyroxene compositions

e ee e e a e a a a a e
 ee c (= 84 86). e
 c ee ave ve 2 c -
 e (e a 0.5%) a e ce ca c -
 ae a a a e (e e-
 e a ae a a e 5ava a ea .// a .
 ca e. / e). ec ee ec -
 ae ave c e ce ca c
 41 4 . , 46 55 . a 1 ▼ .
 (.5a). e -a a e -eae ea e
 acc e 2 3, 2 a 2 c e
 (.5 , c).

4.c. Whole-rock elemental geochemistry

4.c.1. Serpentinites and cumulates

eee e ave ve ()
 (> 12%, c c e e ve e e -
 a)a 2(e a 40%), 2 3(
 e a 1.0%), 2 (0.03 0.06%), a₂ (0.04
 0. 2%)a 2(0.04 0.05%). a e_{2 3} c -

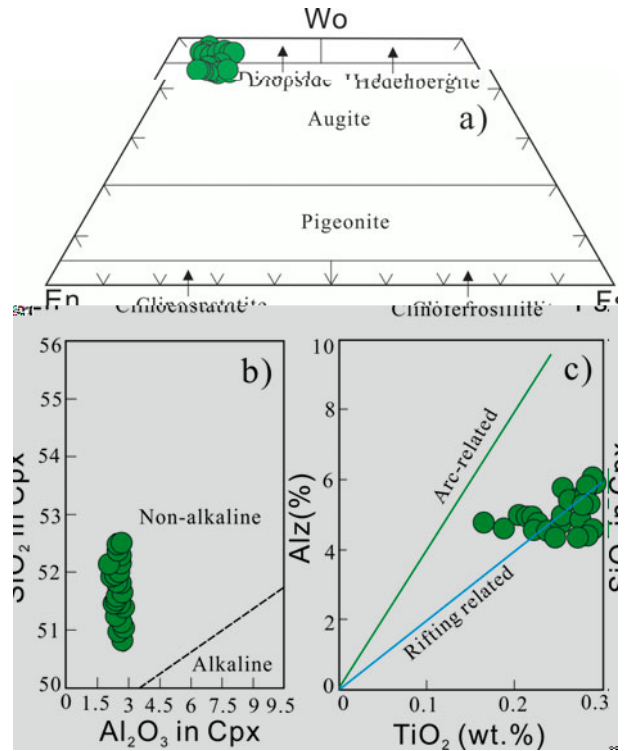


Fig. 5. (a) Ternary diagram of Wo, En, and Fo showing mineral compositions. (b) Scatter plot of Al₂O₃ in Cpx versus TiO₂ (wt.%) showing the field for non-alkaline and alkaline rocks. (c) Scatter plot of Al₂O₃ in Cpx versus TiO₂ (wt.%) showing the field for arc-related and rifting-related rocks.

e e a 8 1(a e 1).
 e a e a a , ca c ea e ee
 . e a ee e e ve (.6).
 e ave ea ve (3 103) a
 c e (5 8) (a e 1). e (> 12%)
 a a₂ , 2 a a c e e c-
 a e a a ea c a ee e a
 c e e a ee e (a , a a) a e
 a e a e e e e e () (e . ,
 a a). eve , ce ee a e c e -
 a , 2 3, e_{2 3} a 2, e
 e a ee a ca e e e e-
 e e e e a a e a . , ee
 ee e ca e e e c e -
 ee . ee e e ave ve a a e e a
 ee e () a - e - e ee e
 () c e (a e 1). eve , e c -
 e - a e c e - a e a e
 (.7), a ea e a e
 ec ee (ea ce, 2014, ec e
 a e ve a e va e a e & c-
 , 1 8).

e a c c ae ave 2 a
 45.87% 51.27%, a a va a e
 e_{2 3} (3.24 4.68%), 2 3 (18.3 1 .6%, e ce
 a e 2013 01-3), a (.54 15.42%), 2
 (0.12 0.34%), a₂ (2. 1 3.38%, e ce a e
 2013 01-3) a 2 (0.11 0.46%) c -
 a ac a a / c a e ec (a e 1).

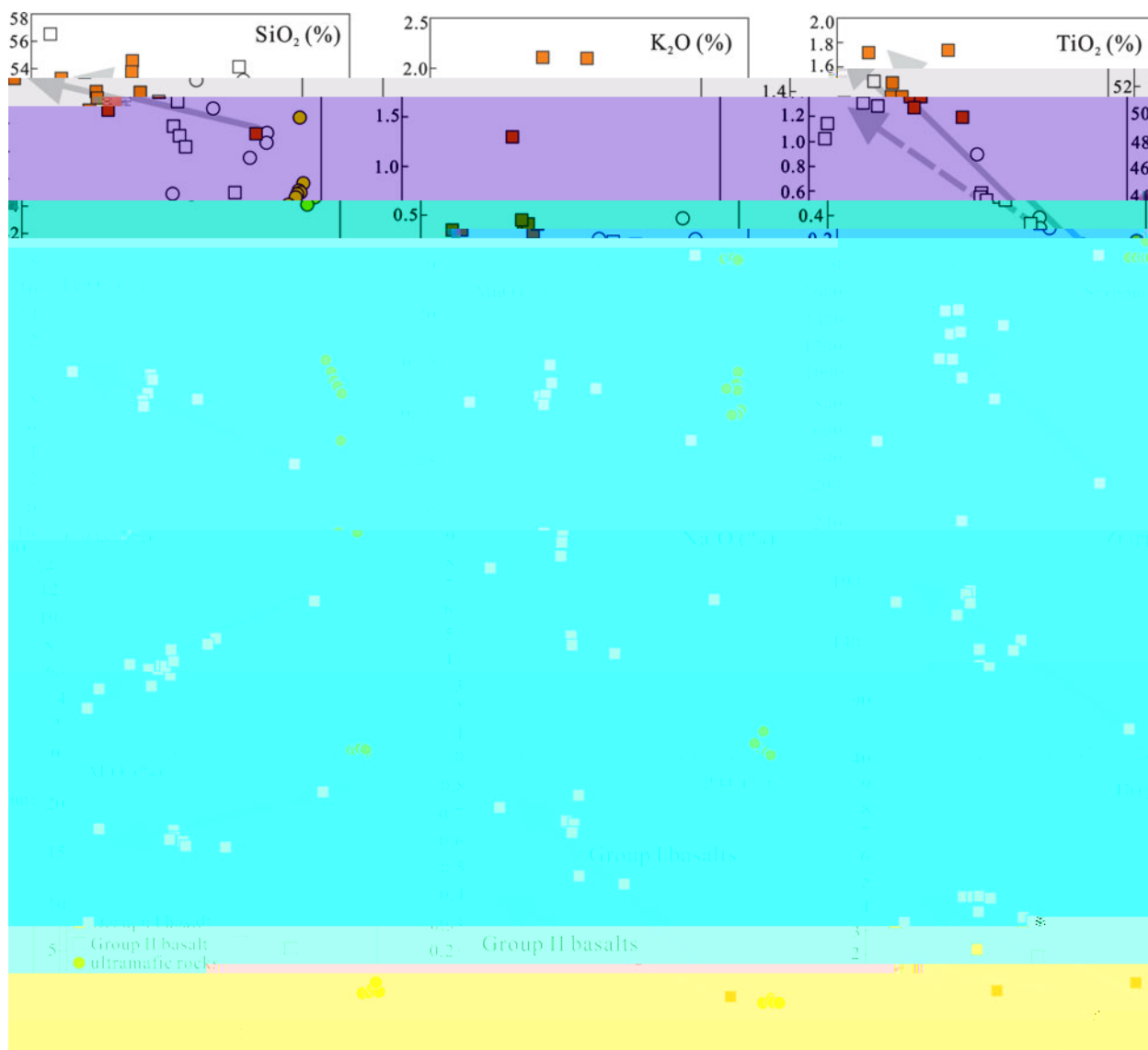


Figure 6. (a) SiO₂ (wt%), (b) K₂O (wt%), and (c) TiO₂ (wt%) concentrations for various rock samples. The plot is divided into horizontal bands representing different rock groups: Group I basalts (top, purple), Group II basalts (middle, cyan), and Group II basalt/ultramafic rock (bottom, yellow). Data points are represented by squares, circles, and triangles. Arrows indicate trends or specific sample locations.

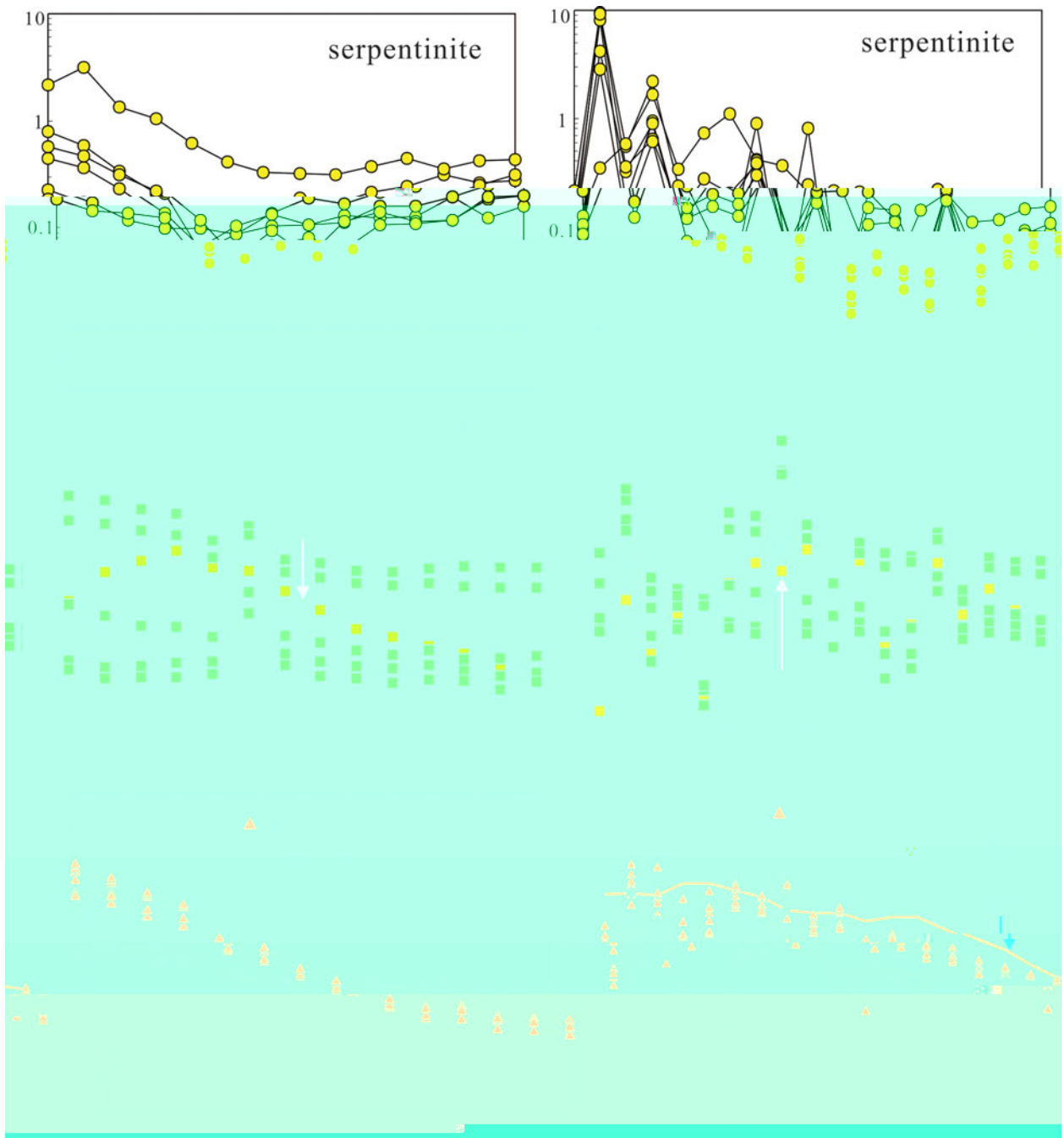
ca c ea e ee . a a-
 ee e a eve e a e a a
 (.6). ec ae ave va a e a c -
 e a 5 41 , a a c -
 e c e- a e a e
 () e c e ((a/) = 1.3 2.8) a
 ce ve a a e (/ = 1.1 2.2).
 a e 2013 01-3 a e a e ,
 e e e ee ec. e e e
 ae eve e -ec . e ve-
 a e () a e c a e e e a-
 a (.7), a ec ae a e c a ace e
 ca e a ve a a e (/ a = 0.2 0.4)
 a va a e vea a e a, a .

4.c.2. Basalts

e a a a a e c a a ave 2 a
 43.15% 57.65% (e a 52%,

a e 1). va a e e a a e a ,
 e c a e e e e ee e
 ca ca . e / v. / 2 a a , e
 aa ca e v e , e. ea-
 a e 1 (1) a a a e 2 (2).
 e 2 a e, a e a e e
 a e ee aa a a e e a a c a -
 e e (.8a). 1 a 2 e a e c
 e ee / v. 2 a a (.8).
 e a e a a , 2, e₂ 3, 2 5, 2, ,
 a cea e e a a 2 3 ec ea e
 ec ea . e 1 a a . e 2
 aa , 2 5, 2, a cea e ee ca
 (.6).

e 1 a a ave e a ve a c -
 e a 124 205 e e 2
 a a ave 50 60 a . 1 a a
 ave e va e (a/) e ee 10 a
 30 (a ve 20) a e a e e a ve

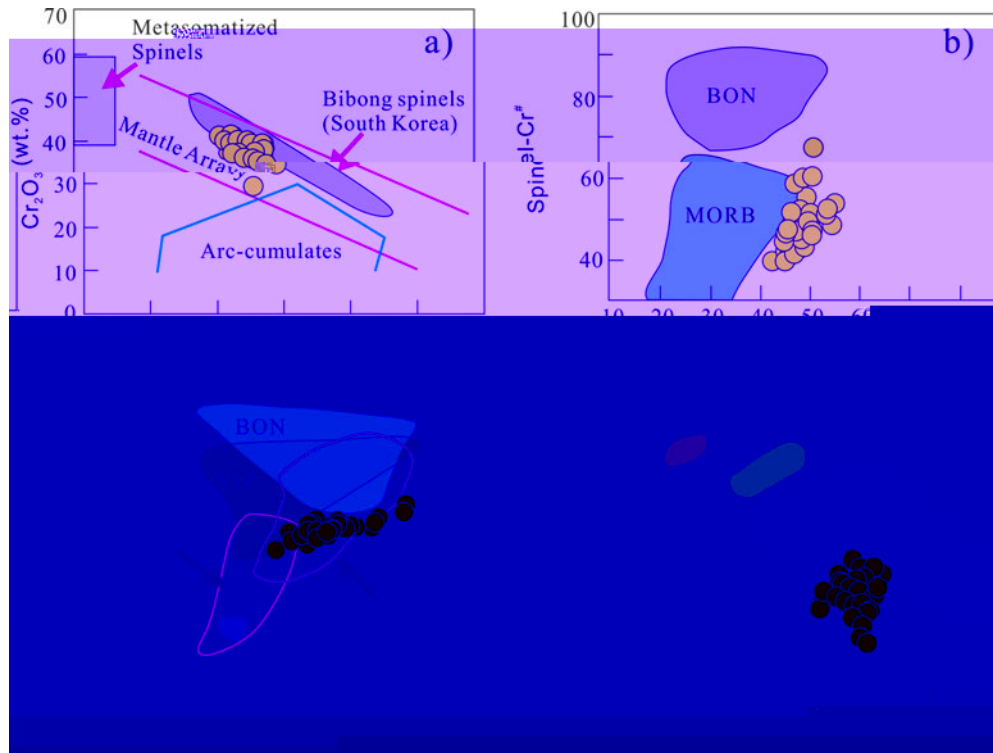


e⁺. (e) e- a e a e a ve a e- a e c a e ace-eee e -
 ee e a a e e e ea a e a ea ea e ev a aa . e a a va e a e
 & c (1 8).

ve a a e (/ = 0.70 1.14)
 (.7). e 2 a a ave ea ve a a -
 e (a/) a 4 6 a
 ve a a e (/ = 1.02 1.21) (.7).
 e - a e -eee a a , e
 1 a a e a e va a e ea -
 ve a a a e / a a 0.44
 0.87, a e a ve ve a a e c -
 e e a a e . e 2 a a ave
 e c a eee e c e a e e
 1 a a a a ce e a ve aa -
 a e ve / a a (~0.11). ee
 ea e ee e e ca c a a (.7).

4. . Whole-rock Sr-N an z rcon Hf-O sotopes

a e cc e
 e ee a ve a a ae e a e 2. 1 a a
 a 2 a a ave a cc -
 . e a a a e ⁸⁷/₈₆ a-
 (0.0024 0.0452) a ⁸⁷/₈₆ a (0.704030
 0.705368), c e ea ve e e
 a ⁸⁷/₈₆ a (0.704015 0.705111, e ce
 2013 03 1). e ave ¹⁴⁷/₁₄₄ a e ee
 0.0 78 a 0.13 4 a ¹⁴³/₁₄₄ a e ee
 0.512707 a 0.51283 a ea c a ε (t) va -
 e +6.3 +7.5 (e ce 2013 03 1 a
 +1.8).



10. (e) c a e c a a a . (a) $2/3 ve$ $2/3 (\%)$ a a (a e a & ,2000). () . $(100 / (+)) ve$ e^{2+} . $(100 e^{2+} / (e^{2+} +))$ e e a e a e (a e a , 1 4, a e & e e ,2001). (c) . $(100 / (+)) ve$. $(100 / (+ e))$ e e a e a e (a e e e *et al.* 1 5). () $2 ve$ $2/3 c$ a e a e e a e a e (a e a e , a & e e ,2001). e , - cea e a a , a- c e a a .

a e (500 480 a) (a *et al.* 2003, *et al.* 2015,), e ev a e a e c a e (430 400 a) (a *et al.* 200 b, 2014 a e e e ce e e) a e a e e c - e (370 350 a) (a *et al.* 2003, *et al.* 2006).

5.b. Or g n of the serpent n te an cumulates

e a a c c ave c e a - e e ve a a e a e e e ca ec c ca a e a v ve a e e a (e e a , & e, 2002, *et al.* 2010

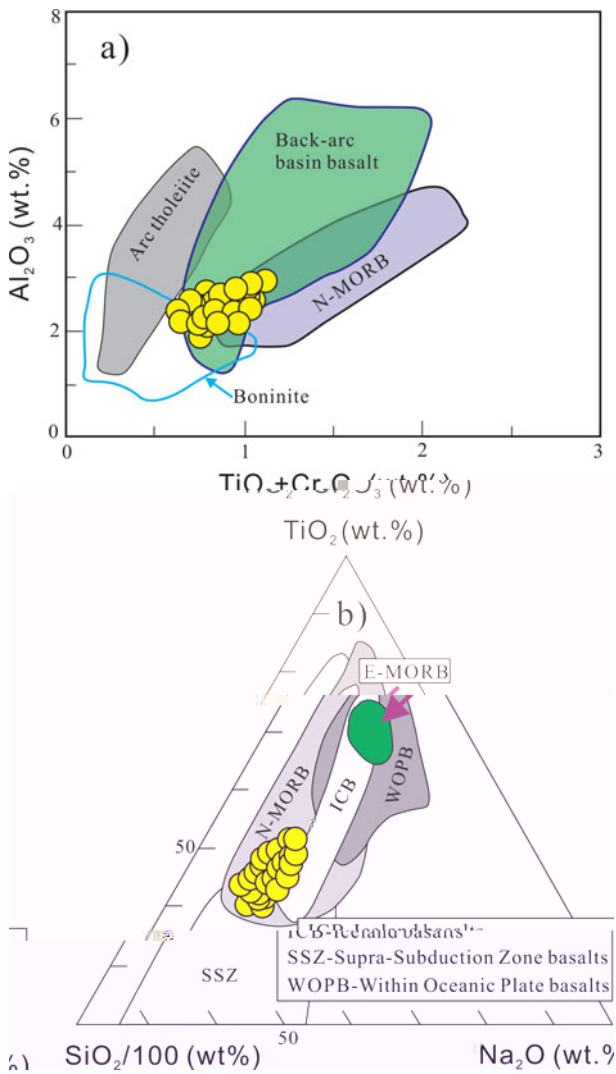


Fig. 11. (a) Al_2O_3 vs. $TiO_2 + Cr_2O_3 + FeO$ diagram for the Zhaheba ophiolite. The fields are defined after (1) Arc tholeiite, (2) Back-arc basin basalt, (3) N-MORB, and (4) Boninite. (b) Ternary diagram of $SiO_2/100$ vs. Na_2O vs. $TiO_2 + Cr_2O_3 + FeO$ for the Zhaheba ophiolite. The fields are defined after (1) E-MORB, (2) N-MORB, (3) ICB, (4) WOPB, and (5) SSZ. The legend defines SSZ as Supra-Subduction Zone basalts and WOPB as Within Oceanic Plate basalts.

... eve, ... c ea e ee / a a / a (.12a), c e ca c a c a a . eve, e e- a e e a e a ec a a a e e a . e e a e a e ce e e c -eae ea a . eve, e / a / a a e a a e e e e -eae ea- a e (.12). ee e, e ca a e a ve a a e ec ee a e ece a eae c -eae ea - a . et al. (2002) ave e a e - ca a e a ve a a e e a e e e a eae c e ec a e ec e ea (c a a e e e e). , e e- ce a e a e ee ac a e a e cea e ee c e c a c a a c -eae ea a .

5.c. Petrogenes s of the Devon an basalts

cc e e ce , e a a a e v e , .e.a a e la e c ca c- a a e 2. 1 a a ave (11 24 , a ve 15), 2 5 (0.4 0.6%) a / a- (11 15, e 60) a va a e (a/) a va e, e e a e -c a a () (ea , ac & , 1 2, - a & e c, 2001) (.13). a e a ve a e ce ave ee e acc e a c ve e ce ca ea e . (1) a a e e ce a ec e cc e a e e e (e. . a , & - a a , 2002), (2) a a e e e c a ea - a e a a e (ea , ac & 1 2, ea & , 1 3, a a et al. 1 6). eae eca e aea a e e e ee e 1 aa . ev e e ae a a e e ve a ccc e - ee ce a e (a , & , 2007, a e et al. 2011). eve, e 1 ave a 87 /86 va e (0.704120 0.706133) a ε (t) va e (+1.8 +7.5). e ae ee e ce . a , e ave e / (3.44 20.4) a e a/ (1.51 2.54) a a (e. . e & a , 1 86). ee e, ee ca ace- c e a a e ce. e ave , e e a e l ae e ve a a e e e ea a e a a e- e e ve a ce a (a a et al. 1 6, e e, 1 6). a e eeae aa ec . e eee ea - e, eeae e eace a ee e eeaea -e ce ce(& e c , 2000). e e e a a a ea ae e e e e ae (ea , ac & , 1 2, a a et al. 1 6). a et al. (2008) e e ev a a a e a e e

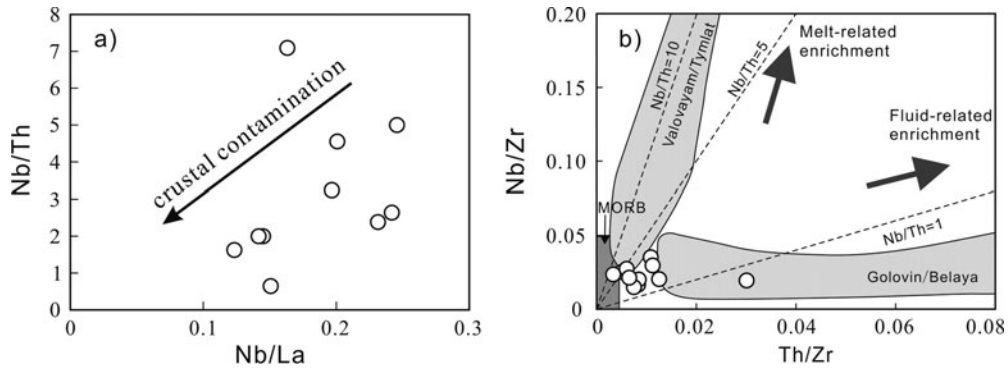


Figure 12. (a) Nb/Th vs Nb/La diagram showing a trend of crustal contamination. (b) Nb/Zr vs Th/Zr diagram showing fields for MORB, Valovayami/Tymjal, Melt-related enrichment (Nb/Th=5), Fluid-related enrichment (Nb/Th=1), and Golovin/Belaya.

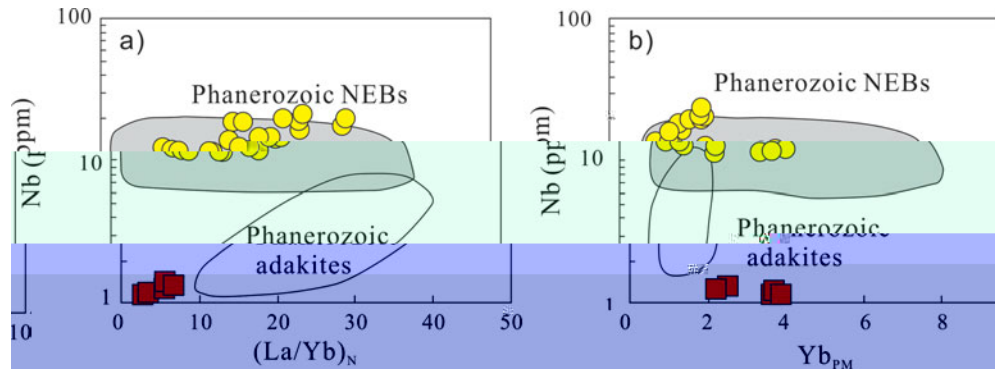


Figure 13. (a) Nb (ppm) vs (La/Yb)_N diagram showing fields for Phanerozoic NEBs and Phanerozoic adakites. (b) Nb (ppm) vs Yb_{PM} diagram showing fields for Phanerozoic NEBs and Phanerozoic adakites.

$\epsilon(t)$ (1.8–1.5) a ($^{87}\text{Sr}/^{86}\text{Sr}$) (0.704120–0.706133) va e, c cae a e ce a c - a ee ee (a e 2). ee a ve $\epsilon(t)$ va e a ($^{87}\text{Sr}/^{86}\text{Sr}$) a cae a e ee a a c a a e a . c e ca a e - a e a a . , e l a a e a e a e e e e e ve a a e a a e e e ev ea a e a a c e e e a e a ce a . e a e e e ca a a c a a e a . e 2 a a ave c e a ea - ve ϵ_2 , a e c e , a / a (< 0.3), / a e / a (.8), e ec e ea a a e ce e a - ee e a / e e ve a a e e ce a (a e , & a e , 1 1, e , 2002). ce a a e ea e a c a a . e e a , e 2 a a ave (/) (0.7–1.0), (a / a) (0.1–0.2) a / (0.6–1.0) a , ca e a e ce e 2 a a a a ea - a e eae cea c c c - (a & c , 1 6). ae e 1 , e 2 a a ave ϵ_2 s c e a / a (/) a (a e 1, .14). e a e e ca a a c v ca c c

(.14). , e 2 a a e ve a a e a a e e e ev ea a e eea e a ce a . e e , e l a 2 a a ae e e e eac e . e e e va cae a e ae ac - ec ce , c c e e e e e e .

5. . Impl cat ons for the Palaeozo c accret on process n eastern Junggar

eeae ee c e eea e a , .e. e ea e e (416 a, et al. 2014, a et al. 2015), a e a a a e (503 485 a, a et al. 2003, et al. 2015,) a e e (400 a) (.1). cc e e eace a e ce e - a a a ea e e (et al. 2014), e ee e - cea ea e a c - eae e . e e ce a e e va eeva a e a a ev a v ca c e e a e e ce a e ea e a e ee - ve e ec c e , c a - cea c a c, ea , acc e a e e, - cea e a ee - ea c (et al. 2007, 200 a,b, a et al. 200 a). ev e a e ec ce a a ca e e e a a - cea c a ac (a et al. 200 b). cc e e e e a

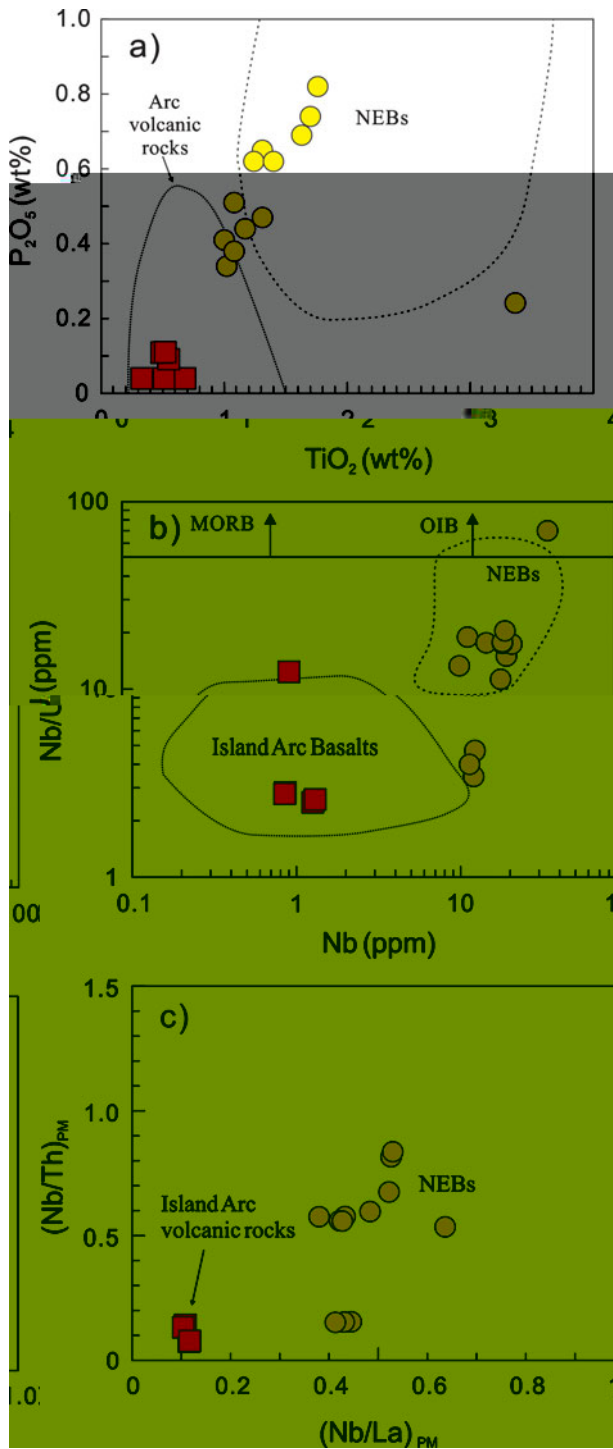


Fig. 14. (a) P_2O_5 vs TiO_2 diagram for the Zhaheba ophiolite. (b) Nb/La vs Nb diagram for the Zhaheba ophiolite. (c) $(Nb/Th)_{PM}$ vs $(Nb/La)_{PM}$ diagram for the Zhaheba ophiolite. The shaded area in (a) represents the field for arc volcanic rocks, and the dashed line represents the field for NEBs. The shaded area in (b) represents the field for Island Arc Basalts. MORB and OIB are Mid-Ocean Ridge Basalt and Ocean Island Basalt, respectively. The shaded area in (c) represents the field for Island Arc volcanic rocks. Data are from *et al.* (1995), *et al.* (2007), *et al.* (2013), *et al.* (2015), and *et al.* (2014).

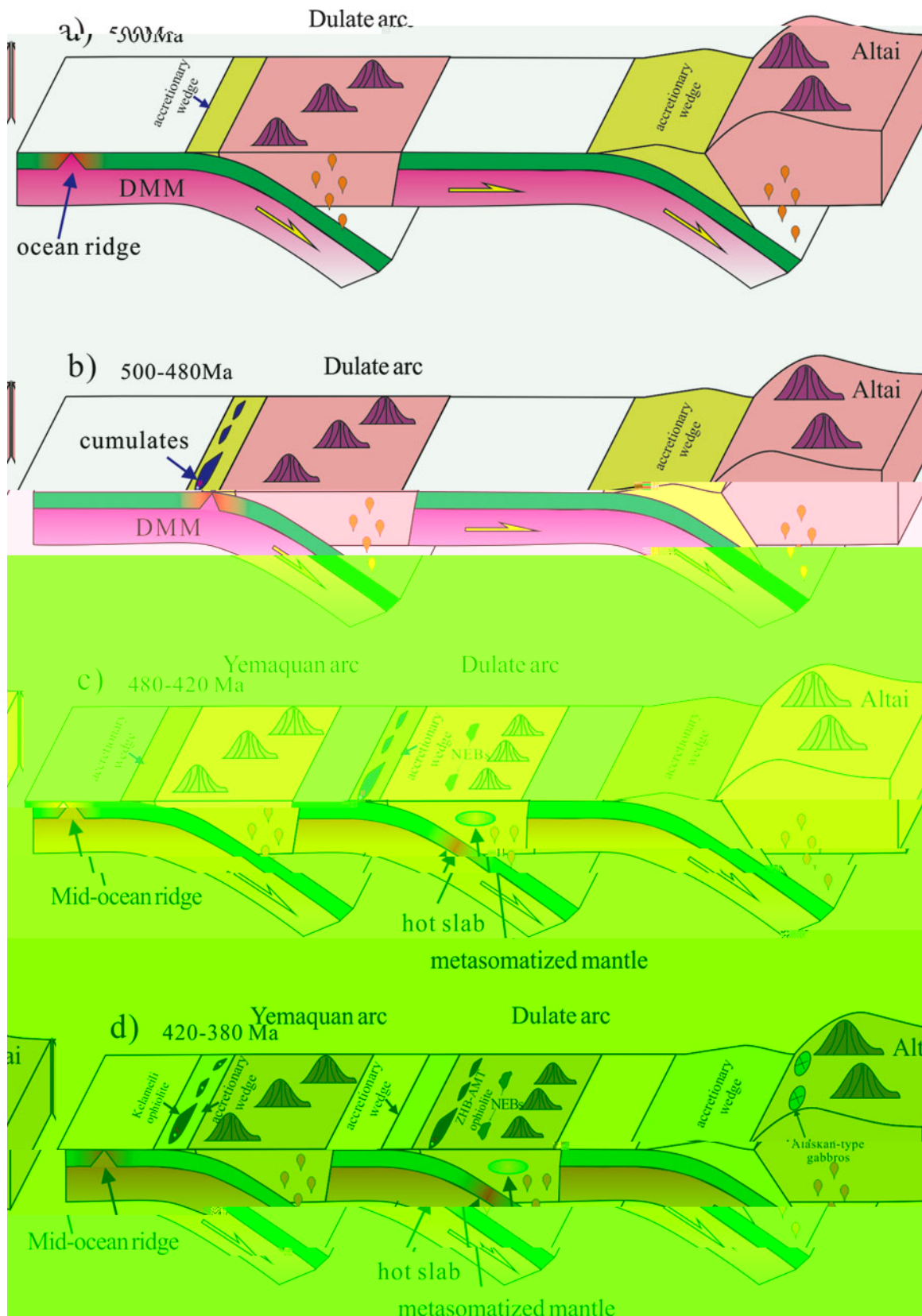
The Zhaheba ophiolite is a typical island arc ophiolite. The arc volcanic rocks are characterized by high P_2O_5 and TiO_2 contents, and low Nb/La and $(Nb/Th)_{PM}$ ratios. The NEBs are characterized by high P_2O_5 and TiO_2 contents, and high Nb/La and $(Nb/Th)_{PM}$ ratios. The Island Arc Basalts are characterized by low P_2O_5 and TiO_2 contents, and low Nb/La and $(Nb/Th)_{PM}$ ratios. The MORB and OIB are characterized by low P_2O_5 and TiO_2 contents, and high Nb/La and $(Nb/Th)_{PM}$ ratios.

The Zhaheba ophiolite is a typical island arc ophiolite. The arc volcanic rocks are characterized by high P_2O_5 and TiO_2 contents, and low Nb/La and $(Nb/Th)_{PM}$ ratios. The NEBs are characterized by high P_2O_5 and TiO_2 contents, and high Nb/La and $(Nb/Th)_{PM}$ ratios. The Island Arc Basalts are characterized by low P_2O_5 and TiO_2 contents, and low Nb/La and $(Nb/Th)_{PM}$ ratios. The MORB and OIB are characterized by low P_2O_5 and TiO_2 contents, and high Nb/La and $(Nb/Th)_{PM}$ ratios.

(1) The Zhaheba ophiolite is a typical island arc ophiolite. The arc volcanic rocks are characterized by high P_2O_5 and TiO_2 contents, and low Nb/La and $(Nb/Th)_{PM}$ ratios. The NEBs are characterized by high P_2O_5 and TiO_2 contents, and high Nb/La and $(Nb/Th)_{PM}$ ratios. The Island Arc Basalts are characterized by low P_2O_5 and TiO_2 contents, and low Nb/La and $(Nb/Th)_{PM}$ ratios. The MORB and OIB are characterized by low P_2O_5 and TiO_2 contents, and high Nb/La and $(Nb/Th)_{PM}$ ratios.

(2) The Zhaheba ophiolite is a typical island arc ophiolite. The arc volcanic rocks are characterized by high P_2O_5 and TiO_2 contents, and low Nb/La and $(Nb/Th)_{PM}$ ratios. The NEBs are characterized by high P_2O_5 and TiO_2 contents, and high Nb/La and $(Nb/Th)_{PM}$ ratios. The Island Arc Basalts are characterized by low P_2O_5 and TiO_2 contents, and low Nb/La and $(Nb/Th)_{PM}$ ratios. The MORB and OIB are characterized by low P_2O_5 and TiO_2 contents, and high Nb/La and $(Nb/Th)_{PM}$ ratios.

(3) The Zhaheba ophiolite is a typical island arc ophiolite. The arc volcanic rocks are characterized by high P_2O_5 and TiO_2 contents, and low Nb/La and $(Nb/Th)_{PM}$ ratios. The NEBs are characterized by high P_2O_5 and TiO_2 contents, and high Nb/La and $(Nb/Th)_{PM}$ ratios. The Island Arc Basalts are characterized by low P_2O_5 and TiO_2 contents, and low Nb/La and $(Nb/Th)_{PM}$ ratios. The MORB and OIB are characterized by low P_2O_5 and TiO_2 contents, and high Nb/La and $(Nb/Th)_{PM}$ ratios.



e 15. (e) a a a e a e e c e e ea e a a e acc e ce
 e a e a e.

(4) $\epsilon_{\text{Nd}}(t)$ values range from -1.14 to -1.02 (420–380 Ma) (Zhang *et al.* 2014, Zhang *et al.* 2015). The $\epsilon_{\text{Nd}}(t)$ values are similar to those of the 2.2 Ga mafic rocks in the Zhaheba ophiolite (Zhang *et al.* 2015). The $\epsilon_{\text{Nd}}(t)$ values are also similar to those of the 2.2 Ga mafic rocks in the Zhaheba ophiolite (Zhang *et al.* 2015). The $\epsilon_{\text{Nd}}(t)$ values are also similar to those of the 2.2 Ga mafic rocks in the Zhaheba ophiolite (Zhang *et al.* 2015).

6. Conclusions

- (1) The 485 Ma mafic rocks in the Zhaheba ophiolite are similar to those of the 400 Ma mafic rocks in the Zhaheba ophiolite.
- (2) The 485 Ma mafic rocks in the Zhaheba ophiolite are similar to those of the 400 Ma mafic rocks in the Zhaheba ophiolite.
- (3) The 485 Ma mafic rocks in the Zhaheba ophiolite are similar to those of the 400 Ma mafic rocks in the Zhaheba ophiolite.

Acknowledgements

This work was supported by the National Natural Science Foundation of China (41176100, 41176101, 41176102, 41176103, 41176104, 41176105, 41176106, 41176107, 41176108, 41176109, 41176110, 41176111, 41176112, 41176113, 41176114, 41176115, 41176116, 41176117, 41176118, 41176119, 41176120, 41176121, 41176122, 41176123, 41176124, 41176125, 41176126, 41176127, 41176128, 41176129, 41176130, 41176131, 41176132, 41176133, 41176134, 41176135, 41176136, 41176137, 41176138, 41176139, 41176140, 41176141, 41176142, 41176143, 41176144, 41176145, 41176146, 41176147, 41176148, 41176149, 41176150, 41176151, 41176152, 41176153, 41176154, 41176155, 41176156, 41176157, 41176158, 41176159, 41176160, 41176161, 41176162, 41176163, 41176164, 41176165, 41176166, 41176167, 41176168, 41176169, 41176170, 41176171, 41176172, 41176173, 41176174, 41176175, 41176176, 41176177, 41176178, 41176179, 41176180, 41176181, 41176182, 41176183, 41176184, 41176185, 41176186, 41176187, 41176188, 41176189, 41176190, 41176191, 41176192, 41176193, 41176194, 41176195, 41176196, 41176197, 41176198, 41176199, 41176200).

Supplementary material

Supplementary material for this article is available at <http://dx.doi.org/10.1017/S0016756816000042>.

References

Zhang, L., Wang, Y., & Li, X. (2014). Age and geochemistry of the Zhaheba ophiolite. *Chemical Geology* **113**, 1–10.

Zhang, L., Wang, Y., & Li, X. (2015). Age and geochemistry of the Zhaheba ophiolite. *Journal of Petrology* **42**, 227–302.

Zhang, L., Wang, Y., & Li, X. (2016). Age and geochemistry of the Zhaheba ophiolite. *Lithos* **97**, 271–88.

Zhang, L., Wang, Y., & Li, X. (2017). Age and geochemistry of the Zhaheba ophiolite. *Geology* **30**, 1071–10.

Zhang, L., Wang, Y., & Li, X. (2018). Age and geochemistry of the Zhaheba ophiolite. *Earth Accretionary Systems in Space and Time* (ed. by Zhang, L., Wang, Y., & Li, X.), pp. 1–36. *Contributions to Mineralogy and Petrology* **181**, 318.

Zhang, L., Wang, Y., & Li, X. (2019). Age and geochemistry of the Zhaheba ophiolite. *Geological Magazine* **139**, 1–13.

Zhang, L., Wang, Y., & Li, X. (2020). Age and geochemistry of the Zhaheba ophiolite. *Geological Society of America Bulletin* **105**, 15–37.

Zhang, L., Wang, Y., & Li, X. (2021). Age and geochemistry of the Zhaheba ophiolite. *Ophiolites* **220**, 1–13.

Zhang, L., Wang, Y., & Li, X. (2022). Age and geochemistry of the Zhaheba ophiolite. *Geology* **21**, 547–50.

Zhang, L., Wang, Y., & Li, X. (2023). Age and geochemistry of the Zhaheba ophiolite. *Journal of Geological Society, London* **149**, 567–71.

Zhang, L., Wang, Y., & Li, X. (2024). Age and geochemistry of the Zhaheba ophiolite. *Contributions to Mineralogy and Petrology* **86**, 54–76.

Zhang, L., Wang, Y., & Li, X. (2025). Age and geochemistry of the Zhaheba ophiolite. *Ophiolites in Earth History* (ed. by Zhang, L., Wang, Y., & Li, X.), pp. 43–68. *Contributions to Mineralogy and Petrology* **123**, 387–411.

Zhang, L., Wang, Y., & Li, X. (2026). Age and geochemistry of the Zhaheba ophiolite. *Chinese Journal of Geology* **50**, 140–54.

Zhang, L., Wang, Y., & Li, X. (2027). Age and geochemistry of the Zhaheba ophiolite. *Contributions to Mineralogy and Petrology* **140**, 283–5.

Zhang, L., Wang, Y., & Li, X. (2028). Age and geochemistry of the Zhaheba ophiolite. *Lithos* **27**, 25–77.

... & ... 2011. *Geological Bulletin of China* **30**, 1508-1513 (in Chinese with English abstract).

... & ... 2011. *Geochimica et Cosmochimica Acta* **75**, 504-512.

... & ... 2001. *Nature* **410**, 67-71.

... & ... 2002. *Chemical Geology* **182**, 22-35.

... & ... 2006. *Journal of Geophysical Research: Solid Earth* (1978-2012) **111**, 11831.

... & ... 2000. *Contributions to Mineralogy and Petrology* **139**, 208-216.

... & ... 2012. *Geological Bulletin of China* **31**, 1267-1278 (in Chinese with English abstract).

... & ... 2014. *Chinese Science Bulletin (Chinese Version)* **59**, 2213-2222.

... & ... 2000. *Transactions of the Royal Society of Edinburgh: Earth Sciences* **91**, 181-193.

... & ... 2010. *Journal of Petrology* **31**, 67-71.

... & ... 2003. *Earth Science Frontier* **10**, 43-56 (in Chinese with English abstract).

... & ... 2001. *Journal of Petrology* **42**, 655-671.

... 2006. *Nature* **380**, 23-40.

... & ... 2000. *Tectonophysics* **326**, 255-268.

... & ... 2010a. *Lithos* **114**, 1-15.

... & ... 2004. *Geological Magazine* **141**, 225-231.

... & ... 2010b. *Geostandards and Geoanalytical Research* **34**, 11-34.

... & ... 2013. *Chinese Science Bulletin* **58**, 464-475.

... & ... 2000. *Lithos* **113**, 274-281.

... & ... 2010. *Chinese Science Bulletin* **55**, 1535-1546.

... 2003. *User's Manual for Isoplot 3.00: A Geochronological Toolkit for Microsoft Excel*. *Earth Science Frontier* **10**, 1-4.

... & ... 2015. *Gondwana Research*, [10.1016/j.gr.2015.04.004](https://doi.org/10.1016/j.gr.2015.04.004).

... 2014. *American Journal of Science* **274**, 32-355.

... & ... 2005. *Geology* **23**, 851-854.

... 2008. *Structure of Ophiolites and Dynamics of Oceanic Lithosphere*. *Journal of Petrology* **38**, 104-114.

... & ... 2000a. *Acta Petrologica Sinica* **25**, 16-24 (in Chinese with English abstract).

... & ... 2000b. *Acta Petrologica Sinica* **25**, 1484-1491 (in Chinese with English abstract).

... & ... 2007. *Acta Petrologica Sinica* **23**, 162-174.

... & ... 2002. *Proceedings of the Ocean Drilling Program, Scientific Results, vol. 176* (eds. ... & ...), 1-60.

, . . . & . . . 2008. c ve e e- cc, e- a c a e a e- e e a e a e a e ca ca ce. *Chinese Science Bulletin* **14**, 2186-2191.

, . . . & . . . 2010. e c a ec c e e v a ce e e a a c e e e e c e a. *Lithos* **117**, 18-208.

, . . . & . . . 2007. e e a c -acc e c e, e e a ec c ev a aca a - a a a- cea c a c- e c e. *Journal of Asian Earth Sciences* **30**, 666-675.

, . . . 2008. e c e ca e cea c a a a ca eca ca a e ea c c ea cea cc. *Lithos* **100**, 14-48.

, . . . 2014. e e e e e - e. *Elements* **10**, 101-108.

, . . . & . . . 2001. a e a a e e, -e c e a a -a e e, a a a e a e- c ea 2.7 a a a ee e e, e v ce, a a a ca a e c ea - c e e e c ce e. *Contribution to Mineralogy and Petrology* **141**, 36-52.

, . . . & . . . 2013. e c e a e e e a - a e (a) ca e e ac e ee a ve, cea c acc e, a - e c e e e e - e cea. *Gondwana Research* **24**, 32-411.

, . . . & . . . 2011. e e e e e e c - e ce e e ce e a a c a a, a - a a e a, e e a a a (e). *Journal of Petrology* **37**, 63-126.

, . . . & . . . 2013. a - c e e a e e, c ca e a c ea a e ec c e a. *Precambrian Research* **231**, 301-324.

, . . . & . . . 2012. e e e c c - c e e e a c a e. *Precambrian Research* **192-195**, 10-208.

, . . . & . . . 2011. e ce e ace e e c c e a a. *Philosophical Transactions of the Royal Society of London* **335**, 311-320.

, . . . & . . . 2011. ca- c e e -ac a e a e e a e e a c a v a. *Nature* **377**, 555-600.

, . . . & . . . 2011. e a ec cc a e a a ae c c a a. *Nature* **364**, 230-231.

, . . . & . . . 2014. a a (~440 a) a a c, a e c a -e c e a a c a v a e e a a e, e a (e e a) a e a a ca c a e e a a e c e. *Lithos* **206-207**, 234-251.

, . . . 2002. c e. *Reviews of Geophysics* **40**, 3-13-38.

, . . . & . . . 200. a a e c e c e e e

a. e a c a e c - c c. *Science in China Series D – Earth Sciences* **52**, 1345-1358.

, . . . & . . . 2018. e ca a c e a c cea c a a. ca a ec a ce e. *Magmatism in the Ocean Basin* (e . . . a e & . . .), .528-48. e ca ce, eca - ca .42.

, . . . & . . . 2008. c a a c e c c e ee a. e ve acc e a e ea e a ae c. *Chemical Geology* **247**, 352-383.

, . . . & . . . 2007. e a e e a ev a a e e a ee a a a ec c ca. *Acta Petrologica Sinica* **23**, 133-144 (ee a ac).

, . . . & . . . 2018. c e ac e e e e va a a a e e. *Contributions to Mineralogy and Petrology* **133**, 1-11.

, . . . & . . . 2006. e ee, a e ae c e c e a a, e a ca e ec cev a acc e a e. *Journal of Geology* **114**, 135-151.

, . . . & . . . 200. c a e ee a a ca c e a e e a a e c e. *Lithos* **110**, 35-12.

, . . . & . . . 2012. e a e a a a ec ca ev a - va ve e e. *Earth-Science Reviews* **113**, 303-341.

, . . . & . . . 2011. e c e ca - e a c ee a a ee a e e e e e e. *Chemical Geology* **20**, 325-343.

, . . . & . . . 2002. e e c ae ce - e a e, a e c a e a a a ec cev. *Journal of Geology* **110**, 1-3.

, . . . & . . . 2006. c ve e e e c a e e a a a ec c ca ce. *Geology in China* **33**, 476-486 (ee a ac).

, . . . & . . . 2014. a e e e e a a (e c e. a a e a (a)? *Geoscience Frontiers* **5**, 525-536.

, . . . & . . . 2008. e a a e a c -e a e acc e a ee a, a ca e ec- cev e a a. *Journal of Asian Earth Sciences* **32**, 102-117.

, . . . & . . . 2013. a e c e acc e a a c a ec c e ee a a e c c a e. *Gondwana Research* **23**, 1316-1341.

, . . . & . . . 2004. a ae c acc e a a c ve e ec c e e a c a e a e a e a. *Journal of Geological Society, London* **161**, 33-42.

- 200 a. - e a e e a c e a e a c e a c e e e e a . - ca e e a c e v , a e c c e a , a e a e e a a . *International Journal of Earth Sciences* **98**, 118–217.
- . . . & , . 200 b. a e c e c - a c c e c e e e e a . *American Journal of Sciences* **309**, 221–70.
- , . 1–3. *Regional Geology of the Xinjiang Uygur Autonomous Region*. e . e ca - e, . 2–145 (e e).
- , . . . & , . 2015. e v a a a - e a a c - a c a a c c e c a e e a e . ca e a e c c e a e e e e a a e c e . *Journal of Asian Earth Sciences* **113**, 75–8.
- , . . . & , . 2012. e a c e a e e e e c e e a e c e ca a e c a e c . *Gondwana Research* **21**, 246–65.
- , . . . & , . 2007. c c e a e e e e e a . a e c a . *Chemical Geology* **242**, 22–3.
- , . . . & , . 2006. a e a a c a a , e a e a (a) . e c e c a c a a c e c a e c c ca . *Acta Geologica Sinica* **80**, 254–63 (e e - a a c).
- & , . 2003. c a a a - a e e e a , a . *Chinese Science Bulletin* **48**, 2231–5.
- , . . . & , . 2013. e c a e a a e . e c e , c e e c , e a ca e e e c a e a . *Lithos* **179**, 263–74.
- , . . . & , . 2012. e v e e c c e . ca e a e c e c e v e a e . *Journal of Asian Earth Sciences* **52**, 117–33.
- , . . . & , . 2008. e c a a e , e a a c a e a e a e - a c e a c . *Acta Petrologica Sinica* **24**, 1054–58 (e e a a c).
- , . . . & , . 1986. e c a e a c . *Annual Review of Earth and Planetary Sciences* **14**, 43–57.